Preprints of the 21st IFAC World Congress (Virtual)
Berlin, Germany, July 12-17, 2020

Speed and torque estimation of variable frequency drives with effective values of stator currents

Y. Kouhi * **J. Müller** * **S. Leonow** * **M. Mönnigmann** *

* *Automatic Control and Systems Theory, Ruhr-Universität Bochum, Universitätsstraße 150, 44801 Bochum, (e-mail: {yashar.kouhi, jens.mueller-r55, sebastian.leonow, martin.moennigmann}@rub.de).*

Abstract: We introduce a new method for torque and speed estimation of induction motors under voltage/frequency (V/f) open-loop control. In contrast to existing approaches that need the phase current, the proposed algorithm only requires the effective value (root mean square) of the stator current and the synchronous frequency, which are usually available from variable frequency inverter (VFI) at no additional cost. Our approach is particularly useful for inverter-fed motor-pumps in which the load varies slowly. We demonstrate the proposed algorithm is able to estimate the pump torque, speed, differential pressure and flow rate in a hydraulic process with a progressive cavity pump.

Keywords: Inverter drives; induction motors; torque motors; speed motors; parameter estimation; positive displacement pumps

1. INTRODUCTION

Variable frequency inverter drives are ubiquitous today. Their use is getting more and more common even in basic and fundamental domains such as hydraulic processes (Ahonen et al. (2013)). A task of the variable frequency inverter (VFI) in these applications is to vary the motor speed in order to achieve the desired flow rate of the pump. A mechanism for the determination of the flow rate of the process is required to meet this control objective. Moreover, in a pumping process often the monitoring of other signals such as pressure, speed, torque, and efficiency of the pump are much desired. Additional measurement device for these signals, even if the installation is physically possible, increases the cost significantly. Consequently, estimation of these quantities based on already existing signals is of great interest. As many VFIs provide information on motor operation, it is natural to engage these data for estimation algorithms.

Speed and torque estimations of an induction motor have been widely studied in the context of electric drives, often for achieving the sensorless control of the motor speed. The most notable algorithms for speed estimation are those that use the equivalent circuit of the induction motor for finding the slip between the synchronous speed and the rotor speed in steady state (Sen (2007)); direct computation of the speed through the estimated rotor flux (Kanmachi and Taahashi (1993)); observer based estimation such as model reference adaptive systems (Kubota et al. (1993)); and anisotropy methods in which the speed is computed by capturing the spatial harmonics of the rotor position on the stator current (Ha and Sul (1999), Holtz (2002)). Once the speed is estimated, the torque estimation can be accomplished with the steady state model (Sen (2007)) or the dynamic model of the motor (Kubota et al. (1993)). All of these approaches require high resolution measurements of the voltage and current of at least one phase of the motor, however.

It is our main contribution to introduce a new method for the computation of the speed and the torque based on the motor model, the effective value of the current, the synchronous speed, and the magnitude of the voltage. The necessary data are usually provided by the VFI and thus no extra sensor is needed. As an application, we employ this approach for the estimation of the torque and speed of a progressive cavity pump driven by an induction motor and use the information of the characteristic curves of the pump to determine the differential pressure and the flow rate of the hydraulic process. It is worth mentioning that using the effective value of the stator current and pump characteristic curves for flow rate estimation of a centrifugal pumping process has already been investigated by Leonow and Mönnigmann (2013). However, in their approach, a model is created from the direct effect of the flow rate on the motor current, and the motor model and parameters do not explicitly appear in the estimation.

In Section 2 we present the motor model and propose our algorithm for the estimation of speed and torque of the induction motor. In Section 3 we introduce the process control system and explain how the differential pressure and the flow rate of the pump can be estimated. Moreover, we verify our algorithm by its implementation on a real test bench. Finally, in Section 4 we give a brief conclusion.

2. COMPUTATION OF SPEED AND TORQUE OF AN INDUCTION MOTOR IN STEADY STATE

The stator model of a three phase induction motor in the rotational coordinate system (d-q) attached to the rotor flux vector is described by the following equations:

Copyright lies with the authors

$$u_{sd} = R_s i_{sd} + \frac{\mathrm{d}\psi_{sd}}{\mathrm{d}t} - \omega_s \psi_{sq}, \tag{1}$$
$$u_{sq} = R_s i_{sq} + \frac{\mathrm{d}\psi_{sq}}{\mathrm{d}t} + \omega_s \psi_{sd}, \tag{2}$$
$$\psi_{sd} = L_s i_{sd} + L_m i_{rd}, \tag{3}$$
$$\psi_{sq} = L_s i_{sq} + L_m i_{rq}, \tag{4}$$

where i_{sd}, i_{sq} and i_{rd}, i_{rq} are the stator and the rotor currents in d and q axes, respectively. Likewise, u_{sd}, u_{sq} and ψ_{sd}, ψ_{sq} describe the stator voltages and the electromagnetic fluxes in the mentioned coordinate frame. The index s always refers to the stator variables and the index r refers to the rotor variables. R_s and R_r represent the resistances, whereas L_s, L_r, and L_m represent the stator, rotor, and mutual inductances, respectively. The parameter

$$\sigma = 1 - \frac{L_m^2}{L_s L_r}. \tag{5}$$

is called leakage factor. Neglecting the motor saturation and assuming that the leakage and mutual inductances are constant, the parameter σ is also constant.

In steady state, the rotor flux coordinate system rotates with the synchronous rotational speed ω_s. In this representation the d-axis current (i_{sd}) builds up the electromagnetic flux ψ_{rd}, and the q-axis current (i_{sq}) is proportional to the electromagnetic torque of the motor. Moreover, the following relations hold in steady state:

$$\frac{\mathrm{d}\psi_{sd}}{\mathrm{d}t} = 0, \ \frac{\mathrm{d}\psi_{sq}}{\mathrm{d}t} = 0, \ i_{rd} = 0, \ i_{rq} = -\frac{L_m}{L_r} i_{sq}, \tag{6}$$

(see, e.g., Quang and Dittrich (2015)). Applying the simplification (6) to (1) and (2), and inserting (3) and (4) in (1) yield

$$u_{sd} = R_s i_{sd} - \omega_s \sigma L_s i_{sq}, \tag{7}$$
$$u_{sq} = R_s i_{sq} + \omega_s L_s i_{sd}. \tag{8}$$

The electromagnetic torque T_e and the shaft torque T_m are related by the momentum equations according to

$$T_e - T_m - F\,\omega_m = J\dot{\omega}_m, \tag{9}$$

where F and J are the friction coefficient and the moment of inertia, respectively, and ω_m represents the mechanical speed in (9). Applying the steady state condition $\dot{\omega}_m = 0$ results in

$$T_m = T_e - F\,\omega_m. \tag{10}$$

Many inverter driven motors operate under the voltage/frequency (V/f) open-loop control to regulate the motor speed. The principle of the V/f control relies on keeping the ratio of the magnitude of voltage vector to frequency, i.e., $|u_s|/|\omega_s|$, constant. The rotor electromagnetic flux ψ_{rd} will then be almost constant and therefore the motor can deliver the nominal torque in the entire basic speed region. From a control systems perspective, we consider the motor under control as a single-input-single-output system, where the synchronous speed represents the control input, the motor speed represents the system output, and the shaft torque is a disturbance. Note that as the magnitude of the voltage is set proportionally to the synchronous frequency by the inverter, this variable is neither control input nor output. We emphasize that under V/f control the motor speed is not exactly equal to the synchronous speed, and a slip (up to 3%) between

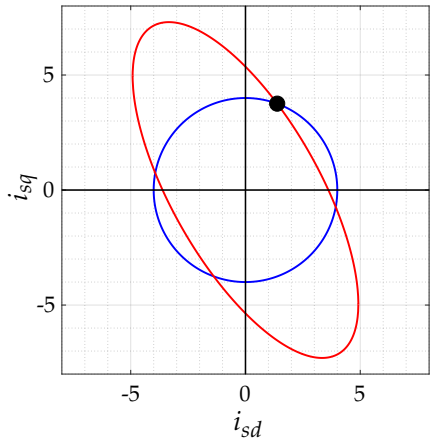

Fig. 1. Curves that specify the currents in d and q axes.

these two variables results depending on the shaft torque. An estimation of the actual motor speed and shaft torque are therefore of obvious interest. We present our estimation algorithm for this purpose in what follows.

2.1 Estimation of motor speed in V/f control

Most VFIs provide the effective value of one phase of stator current I_{eff} as a measurement signal. In our speed estimation algorithm the synchronous rotational speed ω_s serves as the input, I_{eff} is the measured signal, and the actual motor speed ω_m represents the estimation signal. The first step for speed estimation concerns computation of the currents i_{sd} and i_{sq}. Since the current of each phase of the motor in stator-fixed coordinate system is almost sinusoidal in steady state (the effect of higher harmonics of the current caused by the vector modulation is neglected), the magnitude of the current vector $i_s = [i_{sd}\ i_{sq}]^\top$ equals the maximum current of one phase, which is $\sqrt{2}I_{\text{eff}}$. Hence, the mathematical expressions for the magnitude of the I_{eff} and $|u_s|$ read:

$$|u_s| = \sqrt{u_{sq}^2 + u_{sd}^2}, \tag{11}$$
$$I_{\text{eff}} = \frac{\sqrt{2}}{2}\sqrt{i_{sq}^2 + i_{sd}^2}, \tag{12}$$

Combining (7), (8), and (11) results in the following equation for the magnitude of the stator voltage:

$$(R_s i_{sd} - \omega_s \sigma L_s i_{sq})^2 + (R_s i_{sq} + \omega_s L_s i_{sd})^2 = |u_s|^2. \tag{13}$$

Equations (12) and (13) describe a circle and an ellipse in i_{sd} and i_{sq}, respectively, which are illustrated in Figure 1. Since the motor currents are positive in normal operation, we require the intersection point in the first quadrant marked by the black point in Figure 1. The currents i_{sd} and i_{sq} can be computed as follows. Expanding (13) to

$$\begin{aligned}|u_s|^2 = R_s^2(i_{sd}^2 + i_{sq}^2) + 2\omega_s R_s L_s(1-\sigma) i_{sd} i_{sq} + \\ + \omega_s^2 L_s^2(\sigma^2 i_{sq}^2 + i_{sd}^2),\end{aligned} \tag{14}$$

and substituting

$$i_{sd} = \sqrt{2I_{\text{eff}}^2 - i_{sq}^2} \tag{15}$$

results in

$$|u_s|^2 - 2(R_s^2 + \omega_s^2 L_s^2) I_{\text{eff}}^2 = (1-\sigma)\omega_s L_s \Big(2R_s i_{sq} \times \\ \times \sqrt{2I_{\text{eff}}^2 - i_{sq}^2} - \omega_s L_s (1+\sigma) i_{sq}^2 \Big). \quad (16)$$

It proves to be convenient to introduce the auxiliary variables

$$a_1 = 2R_s, \quad a_2 = \omega_s L_s (1+\sigma), \\ a_3 = \frac{|u_s|^2 - 2(R_s^2 + \omega_s^2 L_s^2) I_{\text{eff}}^2}{\omega_s L_s (1-\sigma)}, \quad (17)$$

which permit expressing (16) as

$$a_3 = a_1 i_{sq} \sqrt{2I_{\text{eff}}^2 - i_{sq}^2} - a_2 i_{sq}^2. \quad (18)$$

Rearranging (18) yields

$$\begin{aligned} &(a_3 + a_2 i_{sq}^2)^2 = a_1^2 i_{sq}^2 (2I_{\text{eff}}^2 - i_{sq}^2) \\ &a_3^2 + 2a_3 a_2 i_{sq}^2 + a_2^2 i_{sq}^4 = a_1^2 i_{sq}^2 (2I_{\text{eff}}^2 - i_{sq}^2) \\ &a_3^2 + 2\left(a_3 a_2 - a_1^2 I_{\text{eff}}^2\right) i_{sq}^2 + (a_1^2 + a_2^2) i_{sq}^4 = 0 \\ &i_{sq}^2 = \frac{-a_3 a_2 + a_1^2 I_{\text{eff}}^2 \pm a_1 \sqrt{-2a_3 a_2 I_{\text{eff}}^2 + a_1^2 I_{\text{eff}}^4 - a_3^2}}{a_1^2 + a_2^2}, \end{aligned} \quad (19)$$

where we used $a_1^2 + a_2^2 > 0$ in the last step, which holds since $a_1 > 0$ and $a_2 > 0$ by definition. Furthermore, (18) yields $a_3 + a_2 i_{sq}^2 > 0$, or equivalently,

$$i_{sq}^2 > -a_3/a_2. \quad (20)$$

This implies the solution in the last line of (19) with the positive sign applies. Hence,

$$i_{sq} = \sqrt{\frac{-a_3 a_2 + a_1^2 I_{\text{eff}}^2 + a_1 \sqrt{-2a_3 a_2 I_{\text{eff}}^2 + a_1^2 I_{\text{eff}}^4 - a_3^2}}{a_1^2 + a_2^2}}, \quad (21)$$

$$i_{sd} = \sqrt{\frac{a_3 a_2 + (a_1^2 + 2a_2^2) I_{\text{eff}}^2 - a_1 \sqrt{-2a_3 a_2 I_{\text{eff}}^2 + a_1^2 I_{\text{eff}}^4 - a_3^2}}{a_1^2 + a_2^2}}, \quad (22)$$

where i_{sd} is calculated with (15). The speed of a motor with the number of pole pairs z_p can be calculated from the difference between synchronous speed and the slip speed given by the following equation

$$\omega_m = \frac{1}{z_p}\left(\omega_s - \frac{R_r L_m}{L_r \psi_{rd}} i_{sq}\right) = \frac{1}{z_p}\left(\omega_s - \frac{R_r\, i_{sq}}{L_r\, i_{sd}}\right), \quad (23)$$

(for the derivation of (23) see, e.g., Melkebeek (2018), pp. 678).

2.2 Computation of the motor torque

Assuming the currents i_{sq} and i_{sd} and the speed ω_m are available, the mechanical power P_m of the motor and the shaft torque T_m can be computed. We first model the iron losses in the induction motor to achieve a better accuracy in the estimation of the mechanical power and accordingly the torque. Iron losses P_{Fe} appear in the form of eddy-current losses and hysteresis losses. Since the rotor frequency is much smaller than the stator frequency at the frequencies considered here, the iron losses in rotor can be neglected. The iron losses significantly increase in inverter driven motors due to the harmonic components of the voltages and currents caused by the vector space modulation. These losses are usually modeled by adding a resistance R_{Fe} in the equivalent circuit of the motor parallel to the mutual inductance (see, e.g., Sen (2007)). This resistance is defined by

$$R_{\text{Fe}} = \frac{3}{2}\frac{(\omega_s |\psi_m|)^2}{P_{\text{Fe}}}, \quad (24)$$

where ψ_m is the mutual flux linkage. ψ_m can be expressed in terms of the stator and rotor currents with the formula

$$\psi_m = L_m \left[i_{sd} + i_{rd} \quad i_{sq} + i_{rq} \right]^\top. \quad (25)$$

Subsequently, substituting the rotor currents from (25) by the ones in (6), the magnitude of mutual flux linkage can be determined from the stator currents

$$|\psi_m| = L_m \sqrt{(i_{sd} + i_{rd})^2 + (i_{sq} + i_{rq})^2} \\ = L_m \sqrt{i_{sd}^2 + \frac{L_{r\sigma}^2}{L_r^2} i_{sq}^2}, \quad (26)$$

where $L_{r\sigma}$ is the rotor leakage inductance. It is an established method for the characterization of the iron resistance to run a no-load test and to use the measured values of stator voltages and currents of the three phases and the power factor (Sen (2007)). However, since only the signals provided by the inverter are available in our case, we do not have a direct access to the mentioned signal as a function of time. Thus, we consider a simple approximation for modeling the iron resistance suggested by Quang and Dittrich (2015). The iron resistance can be stated by an expression proportional to the synchronous speed

$$R_{\text{Fe}} = R_{\text{Fe},n} \frac{\omega_s}{\omega_{s,n}}, \quad (27)$$

where $R_{\text{Fe},n}$ is the iron resistance at the nominal frequency $\omega_{s,n}$. We briefly explain how to approximate the parameter $R_{\text{Fe},n}$ from the nominal data of the motor. To this end, we first compute the nominal currents $i_{sd,n}$ and $i_{sq,n}$ with the algorithm from Section 2.1 and the nominal motor data (current, voltage, and synchronous frequency). The nominal mutual flux $\psi_{m,n}$ then results with (26). Next, recalling (6), the iron losses for the nominal operating point equal

$$\begin{aligned} P_{\text{Fe},n} &= P_{\text{elec},n} - P_{m,n} - P_{R_s,n} - P_{R_r,n} - P_{\text{fr},n} \\ &= 3U_n I_{\text{eff},n} \cos(\varphi_n) - P_{m,n} - 3R_s I_{\text{eff},n}^2 + \\ &\quad - \frac{3}{2} R_r \frac{L_m^2}{L_r^2} i_{sq,n}^2 - P_{\text{fr},n}. \end{aligned} \quad (28)$$

We assume the nominal data of the effective value of the voltage of one phase U_n, effective value of stator current $I_{\text{eff},n}$, mechanical power $P_{m,n}$, the power factor $\cos(\varphi_n)$, and the friction losses $P_{\text{fr},n}$ to be available from the motor manufacturer. Thus, by substituting the expression for the iron losses (28) into (24), the iron resistance $R_{\text{Fe},n}$ can be determined. Combining (24), (26), and (27) the iron losses

$$P_{\text{Fe}} = \frac{3}{2}\frac{(\omega_s |\psi_m|)^2}{R_{\text{Fe}}} = \frac{3}{2}\frac{\omega_{s,n}}{R_{\text{Fe},n}} L_m^2 \omega_s \left(i_{sd}^2 + \frac{L_{r\sigma}^2}{L_r^2} i_{sq}^2 \right). \quad (29)$$

result as a function of the frequency ω_s.

Once the iron losses are known, we can compute the air gap power according to the formula

$$P_{\text{ag}} = P_{\text{elec}} - P_{R_s} - P_{\text{Fe}}, \quad (30)$$

where P_{elec} and P_{R_s} indicate the electric power and ohmic losses of the stator, respectively. In the rotor flux coordinate system, they are given by

$$P_{\text{elec}} = \tfrac{3}{2}\, u_s i_s = \tfrac{3}{2}\,(u_{sd}\, i_{sd} + u_{sq}\, i_{sq}), \tag{31}$$

$$P_{R_s} = \tfrac{3}{2}\, R_s\,(i_{sd}^2 + i_{sq}^2). \tag{32}$$

where the currents i_{sd} and i_{sq} results from (21) and (22) and the voltages u_{sd} and u_{sq} result from (7) and (8). In summary,

$$P_{\text{ag}} = \tfrac{3}{2}\left[(1-\sigma)L_s i_{sq} i_{sd} - \frac{L_m^2 \omega_{s,n}}{R_{\text{Fe},n}}\left(i_{sd}^2 + \frac{L_{r\sigma}^2}{L_r^2} i_{sq}^2\right)\right]\omega_s. \tag{33}$$

The friction losses are proportional to the square of the motor speed ω_m according to $P_{\text{fr}} = F\omega_m^2$. Using the following expression for the mechanical power

$$P_m = P_{\text{ag}}(1-s) - P_{\text{fr}}, \tag{34}$$

we can compute the shaft torque as

$$T_m = \frac{P_m}{\omega_m} = \frac{1}{\omega_m}\,(P_{\text{ag}}(1-s) - P_{\text{fr}}) \tag{35}$$

$$= \frac{3}{2} z_p \left[(1-\sigma)L_s i_{sq} i_{sd} - \frac{L_m^2 \omega_{s,n}}{R_{\text{Fe},n}}\left(i_{sd}^2 + \frac{L_{r\sigma}^2}{L_r^2} i_{sq}^2\right)\right] - F\omega_m,$$

for a motor with number of pole pairs z_p, where

$$s = \frac{\omega_s - z_p\,\omega_m}{\omega_s} \tag{36}$$

is the slip parameter.

Table 1 summarizes the steps needed for the computation of the motor speed and torque.

Table 1. Computational steps for estimation of the motor speed and torque.

estimation algorithm:
Required signals and parameters:
• I_{eff} is the measured signal.
• ω_s is the input.
• $\lvert u_s \rvert$ is computed from the V/f table.
• The iron resistance at nominal speed (e.g., derived from (27)) and the motor parameters are required.
Computational steps:
i) Calculate currents i_{sq} from (21) and i_{sd} from (22).
ii) Calculate motor speed from (23).
iii) Calculate motor torque from (35).

3. IMPLEMENTATION AND RESULTS

We apply the proposed algorithm to a test setup with a progressive cavity pump (PCP). We summarize some aspects about the PCP needed for the remainder of the paper in Section 3.1. The proposed algorithm is applied in Section 3.2.

3.1 Inverter-driven progressive cavity pump

Progressive cavity pumps are frequently used in industrial systems for pumping high viscosity and abrasive media (Wittrisch and Cholet (2012), Paladino et al. (2011)). They are not understood as well as centrifugal pumps. We estimate the speed, torque, differential pressure over the pump, and the flow rate, because these quantities are essential for a reliable operation of PCP.

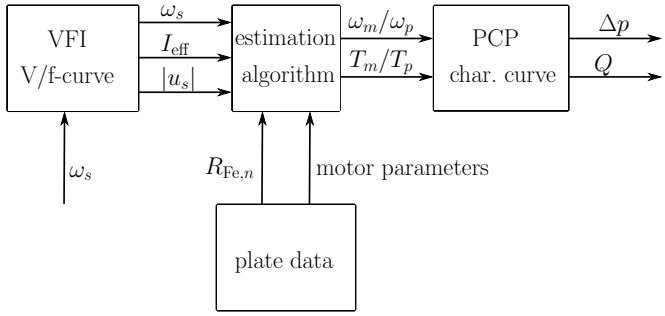

Fig. 2. Block diagram for the estimation.

Figure 2 shows a block diagram of the quantities and their role in the estimation algorithm as applied to the PCP. The PCP is driven by an induction motor. We assume the synchronous frequency is set by the operator of the pump as the input and the effective value of the current is provided by the inverter. The amplitude of the stator voltage is obtained from the V/f table. If the motor resistances and inductances are not known, they can be determined with established algorithms (see, e.g., Quang and Dittrich (2015)). We determined the iron resistance at nominal speed from the motor data provided by the manufacturer as explained in Section 2.2 and estimated the speed and the shaft torque of the motor with the algorithm summarized in Table 1. The estimated motor speed and shaft torque are the input signals to the pump block shown in Figure 2. A gear box with gear ratio γ and efficiency $\eta \leq 1$ is used in our test setup. It can be accounted for in ω_p and T_p with

$$\omega_p = \frac{1}{\gamma}\omega_m, \tag{37}$$

$$T_p = \gamma\,\eta\,T_m. \tag{38}$$

We estimate the differential pressure over the pump with the characteristic curves available from the pump manufacturer. The characteristics that apply in our test case, specifically, the mechanical power (P_p [kW]) as a function of the speed (n [rpm]) for a set of given differential pressures (Δp [bar]) are given by the dashed lines in Figure 3. Since the relationship between the mechanical power P_p and the speed n are linear for the PCP according to Figure 3, the mechanical torque is constant for a constant differential pressure. The mechanical power also is a linear function of the differential pressure for a given speed according to the characteristic curves. Therefore, the torque T_p respects a function of the form

$$T_p = \frac{P_p}{\omega_p} = T_{p,0} + \alpha\Delta p, \tag{39}$$

where $T_{p,0}$ refers to the torque at zero differential pressure and where α can be determined from manufacturer data such as the characteristics shown in Figure 3. The expression (39) can be viewed as a simple form of the torque models for a PCP presented by Moraes-Duzat (2000) and Wittrisch and Cholet (2012). The simple form results if only friction and hydraulic components of the torque are taken into account and the other torque components, e.g. viscous torque, are neglected. In this case $T_{p,0}$ can be considered as the friction torque and the term $\alpha\Delta p$ represents the hydraulic torque, where the constant parameter

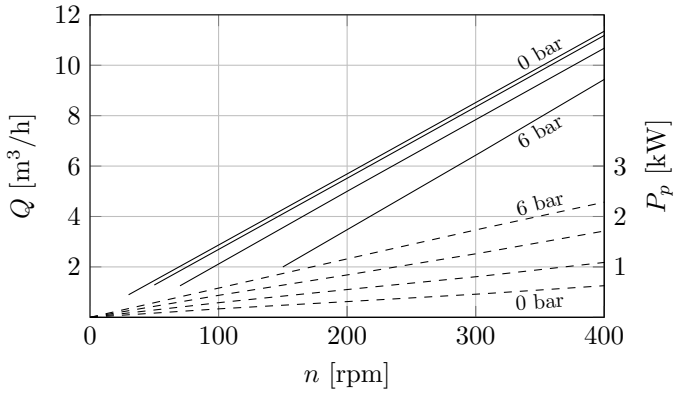

Fig. 3. Characteristic curves for the progressive cavity pump. [1]

α depends on the geometry of the PCP. However, note that the starting torque of a PCP is large (see e.g. Wittrisch and Cholet (2012), pp. 27) and the approximation (39) is only valid for the middle range speeds. We experimentally verified this approximation applies with high accuracy for the estimation of the torque in the range of 100-400 rpm.

The values $T_{p,0} = 15.03$ and $\alpha = 5.97$ apply in our test setup. After determining T_p with (38), the differential pressure can be determined with (39). Subsequently, we determine the flow rate with the characteristic curve available from the pump manufacturer. This second characteristic curve, which states the flow rate Q as a function of the speed n for fixed differential pressures Δp, is given in Figure 3 (solid lines). For our specific test setup, a characteristic curve corresponding to a differential pressure $\Delta p\,[\mathrm{bar}] \in \{0, 2, 4, 6\}$ can be approximated by

$$Q(t) = Q_{n_{\mathrm{ref}},\Delta p} + k_{n_{\mathrm{ref}},\Delta p}(n(t) - n_{\mathrm{ref}}), \tag{40}$$

where $Q_{n_{\mathrm{ref}},\Delta p}\,[\mathrm{m}^3/\mathrm{h}] \in \{2.9, 2.72, 2.15, 0.536\}$ is the flow rate value corresponding to the reference speed $n_{\mathrm{ref}}\,[\mathrm{rpm}] = 100$ and $k_{n_{\mathrm{ref}}} \in \{0.0283, 0.0283, 0.0285, 0.0298\}$. The flow rate $Q(t)$ corresponding to a differential pressure $\Delta p \in [\Delta p_1, \Delta p_2]$ at a speed $n(t)$, where $\Delta p_1 = 2\lfloor \frac{\Delta p}{2} \rfloor$ and $\Delta p_2 = 2\lfloor \frac{\Delta p}{2} \rfloor + 2$ ($\lfloor \cdot \rfloor$ is the floor operator) can be computed in the following way. We obtain the variable $Q_1(t)$ by inserting $n(t)$, $Q_{n_{\mathrm{ref}},\Delta p_1}$, and $k_{n_{\mathrm{ref}},\Delta p_1}$ in (40). Analogously, the variable $Q_2(t)$ is computed at the same speed with the differential pressure Δp_2. Then, the flow rate $Q(t)$ can be calculated by the linear interpolation of $Q_1(t)$ and $Q_2(t)$ as

$$Q(t) = \theta\, Q_1(t) + (1 - \theta) Q_2(t), \tag{41}$$

where the parameter $0 \le \theta \le 1$ is defined by

$$\theta = \frac{\Delta p_2 - \Delta p}{2}. \tag{42}$$

3.2 Results

Figure 2 shows a sketch of the experimental setup. The fluid pumped from the container a) passes through the PCP b) and the control valve c), and eventually flows back to the container a). The control valve produces a back pressure, allowing the realization of different operational points. The PCP is driven by an induction motor [2]. The iron resistance at nominal operating point is approximated by (27), where for this case $R_{\mathrm{Fe},n} = 628\,\Omega$ has been calculated. The motor and pump are connected via a gear box with the transmission ratio $\gamma = 2.94$ and the efficiency $\eta = 0.96$. By using the algorithm introduced in Quang and Dittrich (2015) (pp. 207), we determined the motor parameters

$$R_s = R_r = 1.16\Omega,\ L_m = 0.16\,\mathrm{H},$$
$$L_s = L_r = 0.19\,\mathrm{H},\ \sigma = 0.0812 \tag{43}$$

from the nominal data. The friction coefficient of the shaft is taken from the motor manufacturer data sheet as $F = 7.69 \times 10^{-4}$. The VFI is set to V/f open loop mode. We record the pump speed, torque, flow rate, and pressure signals of the pump separately by additional sensors for verification purposes. Note that these additional sensors are not used for the proposed algorithm. All data is recorded with the sampling time 1 ms.

Starting from the synchronous frequency 10 Hz, we increment the motor synchronous frequency by steps of 10 Hz every 30 s. The position of the control valve c) is kept constant. Figure 5 shows the estimated current signals i_{sd} and i_{sq}, and the measured signal I_{eff}. The flux producing current i_{sd} is almost constant as expected, whereas the

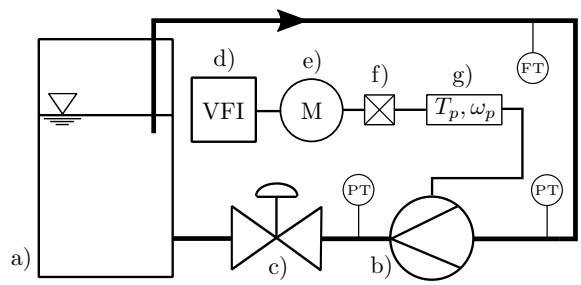

Fig. 4. Components of the pumping process test setup: a) container; b) PCP; c) control valve; d) VFI; e) induction motor; f) gear box. Measurement devices: g) torque and speed transmitter; PT: pressure transmitter; FT: flow transmitter.

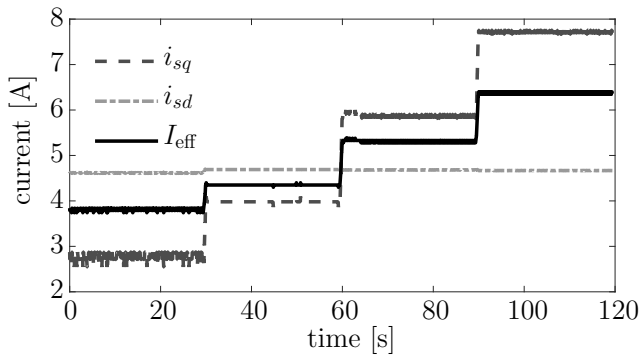

Fig. 5. Estimation of the currents i_{sd} and i_{sq}.

[1] 10-6L manufactured by Seepex GmbH with undersize rotor.

[2] SK-112MH/4 manufactured by Nord GmbH. Nominal data: power 4 KW, current 8A in star connection, frequency $f_n = 50$ Hz, effective voltage of one phase with respect to the star connection point $U_n = 230$ V, speed $n_n = 1440$ rpm, power factor $\cos\varphi_n = 0.83$, and number of pole pairs $z_p = 2$.

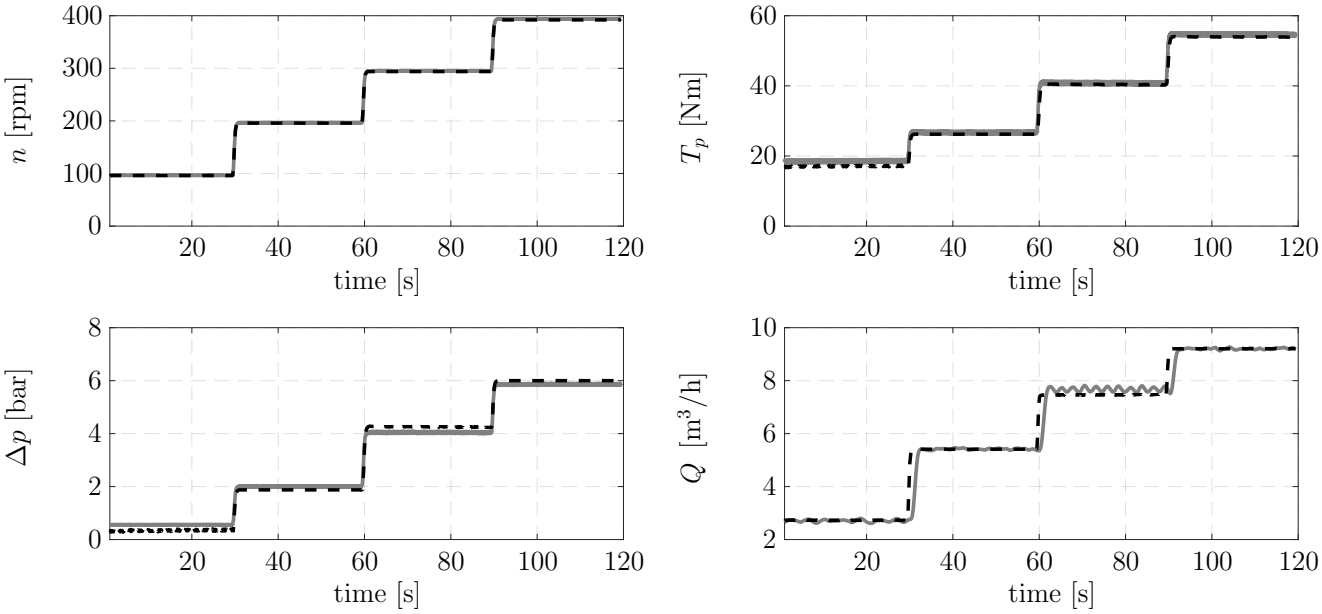

Fig. 6. Estimation signals (dashed) and reference measurements (solid) for the PCP process.

torque producing current i_{sq} changes due to the load changes. Figure 6 depicts the estimated signals, in which the pressure and the flow signals are calculated from the characteristic curves given by Figure 3. All signals in this picture are filtered by a first order low pass filter with the time constant of 0.2 s for the sake of an easier comparison.

It is evident that the proposed algorithm results in a high accuracy. Specifically, the maximum range of the errors remain within the following bounds: 2 rpm for speed estimation, 1 Nm for torque estimation, 0.1 bar for pressure estimation, and $0.2\,\mathrm{m}^3/\mathrm{h}$ for flow rate estimation.

4. CONCLUSION

We developed an algorithm for the speed and torque estimation of an induction motor in steady state. This algorithm is suited for applications in which the motor operates under V/f open loop control when only effective stator current is available. In particular, the proposed algorithm does not require phase currents. We demonstrated the viability of the proposed algorithm with a torque, speed, differential pressure and flow rate estimation for a progressive cavity pump. In this estimation scheme the effective value of the stator current is indeed the only signal that must be measured online to estimate all process signals. This method is simple and exhibits high accuracy results in practical implementations.

ACKNOWLEDGEMENTS

The authors gratefully acknowledge the Ministerium für Wirtschaft, Innovation, Digitalisierung und Energie des Landes Nordrhein-Westfalen for funding this project.

Ministerium für Wirtschaft, Innovation, Digitalisierung und Energie des Landes Nordrhein-Westfalen

REFERENCES

Ahonen, T., Tamminen, J., Ahola, J., Niinimäki, L., and Tolvanen, J. (2013). Sensorless estimation of the pumping process characteristics by a frequency converter. In *Proceedings of the 15th European Conference on Power Electronics and Applications (EPE)*, 1–10.

Ha, J. and Sul, S. (1999). Sensorless field-orientation control of an induction machine by high-frequency signal injection. *IEEE Transactions on Industry Applications*, 35(1), 45–51.

Holtz, J. (2002). Sensorless control of induction motor drives. *Proceedings of the IEEE*, 90(8), 1359–1394.

Kanmachi, T. and Taahashi, I. (1993). Sensor-less speed control of an induction motor with no influence of secondary resistance variation. In *Conference Record of the IEEE Industry Applications Conference Twenty-Eighth IAS Annual Meeting*, volume 1, 408–413.

Kubota, H., Matsuse, K., and Nakano, T. (1993). DSP-based speed adaptive flux observer of induction motor. *IEEE Transactions on Industry Applications*, 29(2), 344–348.

Leonow, S. and Mönnigmann, M. (2013). Soft sensor based dynamic flow rate estimation in low speed radial pumps. In *Proceedings of the European Control Conference (ECC)*, 778–783.

Melkebeek, J.A. (2018). *Electrical Machines and Drives: Fundamentals and Advanced Modelling.* Power Systems. Springer.

Moraes-Duzat, R. (2000). *Analytical and experimental investigation of photovoltaic pumping systems.* Ph.D. thesis, Universität Oldenburg.

Paladino, E., Lima, J., Pessoa, P., and Almeida, R. (2011). A computational model for the flow within rigid stator progressing cavity pumps. *Journal of Petroleum Science and Engineering*, 78(1), 178–192.

Quang, N. and Dittrich, J. (2015). *Vector Control of Three-Phase AC Machines: System Development in the Practice.* Springer, Berlin Heidelberg.

Sen, P. (2007). *Principles of electric machines and power electronics.* Wiley India Pvt. Limited.

Wittrisch, C. and Cholet, H. (2012). *Progressing Cavity Pumps: Oil Well Production Artificial Lift.* Editions Technip.